

# A Deep-Genetic Algorithm (Deep-GA) Approach for High-Dimensional Nonlinear Parabolic Partial Differential Equations

Endah RM Putri<sup>a,\*</sup>, Muhammad L Shahab<sup>b,a</sup>, Mohammad Iqbal<sup>a</sup>, Imam Mukhlash<sup>a</sup>, Amirul Hakam<sup>a</sup>, Lutfi Mardianto<sup>c</sup>, Hadi Susanto<sup>b</sup>

<sup>a</sup>*Department of Mathematics, Faculty of Science and Data Analytics, Institut Teknologi Sepuluh Nopember, Jl. Raya ITS, Sukolilo, Surabaya, 60111, Indonesia*

<sup>b</sup>*Department of Mathematics, Khalifa University, Abu Dhabi, PO Box 127788, United Arab Emirates*

<sup>c</sup>*Department of Mathematics, Institut Teknologi Sumatera, Jl. Terusan Ryacudu, Way Hui, Jati Agung, Lampung Selatan, 35365, Indonesia*

---

## Abstract

We propose a new method, called a deep-genetic algorithm (deep-GA), to accelerate the performance of the so-called deep-BSDE method, which is a deep learning algorithm to solve high dimensional partial differential equations through their corresponding backward stochastic differential equations (BSDEs). Recognizing the sensitivity of the solver to the initial guess selection, we embed a genetic algorithm (GA) into the solver to optimize the selection. We aim to achieve faster convergence for the nonlinear PDEs on a broader interval than deep-BSDE. Our proposed method is applied to two nonlinear parabolic PDEs, i.e., the Black-Scholes (BS) equation with default risk and the Hamilton-Jacobi-Bellman (HJB) equation. We compare the results of our method with those of the deep-BSDE and show that our method provides comparable accuracy with significantly improved computational efficiency.

*Keywords:* high dimensionality, non-linear equations, genetic algorithm, backward stochastic differential equation

---

## 1. Introduction

Many natural phenomena and complex systems are modeled by parabolic partial differential equations (PDEs), particularly in financial industry such as derivative pricing and portfolio optimization models. Nonlinear parabolic PDEs such as the Black-Scholes (BS) with default risk and the Hamilton-Jacobi-Bellman (HJB) equations are popular examples of PDEs in the field [1], while other examples of nonlinear parabolic PDEs can be found in [2, 3, 4, 5]. Nonlinearity in the models aims to incorporate phenomena like default risks [6], transaction costs [7], and stochastic volatilities [8]. As most nonlinear

---

\*Corresponding author

*Email address:* endahrmp@matematika.its.ac.id (Endah RM Putri)

models have no analytical solution, approximation or numerical methods are required. Adding high-dimensionality to the nonlinear financial models increases the complexity of the solution process [9]. Moreover, high-dimensional nonlinear models bring the so-called curse of dimensionality (CoD) as extensive and complex computations grow exponentially. Classical grid based methods i.e., finite difference [10, 11], finite element [12], or finite volume methods [13], fail in high dimensional cases and work only in the lower one or two dimensions [9].

Monte Carlo method is a powerful alternative to obtain accurate solutions of high dimensional problems where CoD exists. In general, the method employs random simulations to generate all possible solutions and determines the optimal one. It is then applied to linear PDEs in the form of Kolmogorov backward problems. After a slow development of the algorithm, a multilevel Picard approximation method (MLP) made a break through [9] as a nonlinear Monte Carlo approximation method. Under certain assumptions, the MLP was proven analytically to solve CoD in nonlinear PDEs [14].

The so-called deep-BSDE algorithm has been recognized as the first deep learning based method [1, 15, 16] in solving high dimensional semi-linear parabolic PDEs. The method represents the PDEs, through their corresponding backward stochastic differential equations (BSDEs), as a deep learning (stochastic optimization) problem that finds an optimal initial guess satisfying a given terminal condition. The deep learning based method is applicable to various high-dimensional complex problems, such as an optimal stopping problem [17, 18], a fixed point problem [19], a many-electron Schrödinger equation as an eigenvalue problem [20], etc. Accordingly, the method has been extended in several directions, such as into least square based deep learning method for not only semi-linear PDEs but also general PDEs [21], deep-BSDE using second order BSDEs for fully nonlinear PDEs [22], deep splitting method for parabolic PDEs which separate the linear and nonlinear terms to save the computational time [23], etc.

The aforementioned studies commonly employ a predetermined initial guess, which we assume comes from a trial and error process. However, we argue that appropriately selecting the initial guess is crucial and can contribute to a faster convergence, as we will demonstrate in Section 4 below. Here, we propose to employ a genetic algorithm (GA) to achieve the advantages. Pan et al. [24] found that employing both GA and gradient descent algorithms enables a faster global search for optimal weights in neural networks. They also conclude that the use of GA outperforms other evolutionary algorithms, such as a differential evolution and a particle swarm optimization. Ding et al. [25] showed that combining GA and a gradient descent algorithm produces better solutions and has a good and stable performance. As an example to applications in PDEs, a hybrid deep learning and GA for data-driven discovery of PDEs is presented in [26]. Moreover, GA is applicable to many areas [27, 28, 29, 30, 31, 32].

Instead of relying on a fixed initial guess, we present a deep-genetic algorithm (deep-GA) method that fuses GA with the Adam optimizer to address the original deep learning problem discussed in [1]. The learning process of the deep-GA, involving weight updates, is divided alternately between GA and the Adam optimizer. The primary objective of this research is to develop an efficient method for solving the deep learning problem emerging from high-dimensional nonlinear parabolic PDEs.

This paper is organized as follows. Section 2 presents the governing equations including the set-up of the PDEs and BSDEs of the nonlinear BS and HJB equation. We will also revisit the deep-BSDE method. Section 3 discusses the set-up of GA in the

BSDE equation and the method in [1]. Simulation results and discussions are provided in Section 4. Finally, conclusion is given in Section 5.

## 2. Mathematical equations

Solving high-dimensional nonlinear parabolic PDEs is known for their CoD. We consider a general form of the class of equations and its relation to BSDE [1]. We will give a brief description about the solution process of the typical PDE.

In this paper, we consider two PDEs, namely a nonlinear BS equation with default risk, and the HJB equation that arises when considering a classical linear-quadratic Gaussian (LQG) control problem [1]. These two equations will serve as test beds for our method. For the reader's convenience, a concise explanation of the two equations is provided in this section.

### 2.1. Backward Stochastic Differential Equations (BSDEs)

We are interested the following class of nonlinear parabolic PDEs [1]

$$\begin{aligned} \frac{\partial u}{\partial t}(t, x) + \frac{1}{2} \text{Tr}(\sigma \sigma^\top(t, x)(\text{Hess}_x u)(t, x)) + \nabla u(t, x) \cdot \mu(t, x) \\ + f(t, x, u(t, x), \sigma^\top \nabla u(t, x)) = 0, \end{aligned} \quad (1)$$

with a terminal condition  $u(T, x) = g(x)$  for  $x = \{x_1, x_2, \dots, x_d\}$  and time  $t$ . A volatility function  $\sigma(t, x)$  is a  $d \times d$  matrix-valued function,  $\mu(t, x)$  is a known vector-valued function,  $\sigma^\top(t, x)$  is the transpose of  $\sigma(t, x)$ ,  $\text{Hess}_x u$  denotes the Hessian of function  $u(t, x)$  with respect to  $x$ ,  $\text{Tr}$  is the matrix trace, and  $f(\cdot)$  is a given nonlinear function. The aim is to find the solution  $u(0, X_0)$  at  $t = 0$  and  $x = X_0 \in \mathbb{R}^d$ .

Let  $\{X_t\}_{t \in [0, T]}$  be a stochastic process in  $d$  dimension which satisfies

$$X_t = X_0 + \int_0^t \mu(s, X_s) ds + \int_0^t \sigma(s, X_s) dW_s, \quad (2)$$

where  $\{W_t\}_{t \in [0, T]}$  is a Brownian motion (Wiener process). The solution of Eq. (1) satisfies the following BSDE [33]

$$\begin{aligned} u(t, X_t) = u(0, X_0) - \int_0^t f(s, X_s, u(s, X_s), \sigma^\top(s, X_s) \nabla u(s, X_s)) ds \\ + \int_0^t [\nabla u(s, X_s)]^\top \sigma(s, X_s) dW_s. \end{aligned} \quad (3)$$

To solve Eq. (3) for  $u(0, X_0)$  numerically, one normally employs a temporal discretization to partition the time interval  $[0, T]$  into  $0 = t_0 < t_1 < \dots < t_N = 1$ . A simple Euler scheme is then applied to obtain

$$X_{t_{n+1}} \approx X_{t_n} + \mu(t_n, X_{t_n}) \Delta t_n + \sigma(t_n, X_{t_n}) \Delta W_n \quad (4)$$

and

$$\begin{aligned} u(t_{n+1}, X_{t_{n+1}}) \approx u(t_n, X_{t_n}) - f(t_n, X_{t_n}, u(t_n, X_{t_n}), \sigma^\top(t_n, X_{t_n}) \nabla u(t_n, X_{t_n})) \Delta t_n \\ + [\nabla u(t_n, X_{t_n})]^\top \sigma(t_n, X_{t_n}) \Delta W_n \end{aligned} \quad (5)$$

where

$$\Delta t_n = t_{n+1} - t_n, \quad \Delta W_n = W_{t_{n+1}} - W_{t_n} \quad (6)$$

for  $n = 1, \dots, N - 1$ .

## 2.2. Non-linear Black-Scholes equation with default risk

A standard BS equation is a linear parabolic PDE that becomes nonlinear when default risk is incorporated. The nonlinearity in these PDEs leads to challenges in obtaining analytical solutions. The complexity of these PDEs increases with the presence of multi-assets in financial products combined with the nonlinear nature of the problem. The BS equation for a multi-asset European contingent claim with default risks is explained in the following.

Let  $u(t, x)$  be the fair price function of a multi-asset European contingent claim with default risks in  $d$  dimension and time  $t$ , where the  $d$ -dimensional underlying assets are represented by  $x = \{x_1, x_2, \dots, x_d\}$ . We refer to a general form of a nonlinear PDE in Eq. (1) for the financial contract model. We define  $\sigma(t, x) = \hat{\sigma} \text{diag}(x)$  and  $\mu(t, x) = \hat{\mu}x$  where  $\hat{\sigma}$  and  $\hat{\mu}$  are known constant volatility and drift of the contingent claim return, respectively.

The nonlinear part of the equation is represented by a default risk function  $Q(u(t, x))$  which relies on the fair price of a contingent claim function  $u(t, x)$ . The terms  $v^h$  and  $v^l$  denote rate of default risks for high and low thresholds of the contingent claim's fair price  $u(t, x)$ , respectively. It is assumed that  $v^h < v^l, \gamma^h > \gamma^l$ , and a recovery rate  $\delta \in [0, 1]$ . The function is modeled as a first jump of the Poisson process in a possible default within three regions: high risk  $(-\infty, v^h)$ , moderate risk  $[v^h, v^l]$ , and low risk  $(v^l, \infty)$ . The value of default risk  $Q(u(t, x))$  is equal to  $\gamma^h$  if the contingent claim price  $u(t, x) < v^h$  or falls in the high risk region. Conversely,  $u(t, x) > v^l$  or falls in the low risk region, the value of  $Q(u(t, x))$  is  $\gamma^l$ . In region  $[v^h, v^l]$ , the value of  $Q(u(t, x))$  is classified as moderate risk and is obtained by an interpolation of the default risk  $Q(u(t, x))$  in the high risk and low risk regions.

The nonlinear BS equation with default risk as the model of the contingent claim can be written as

$$\begin{aligned} \frac{\partial u}{\partial t}(t, x) + \hat{\mu}x \cdot \nabla u(t, x) + \frac{\hat{\sigma}^2}{2} \sum_{i=1}^d |x_i|^2 \frac{\partial^2 u}{\partial x_i^2}(t, x) \\ + f(t, x, u(t, x), \sigma^T \nabla u(t, x)) = 0 \end{aligned} \quad (7)$$

where

$$f(t, x, u(t, x), \sigma^T \nabla u(t, x)) = -(1 - \delta)Q(u(t, x))u(t, x) - ru(t, x)$$

with

$$\begin{aligned} Q(u(t, x)) = \mathbb{1}_{(-\infty, v^h)}(u(t, x))\gamma^h + \mathbb{1}_{[v^l, \infty)}(u(t, x))\gamma^l \\ + \mathbb{1}_{[v^h, v^l)}(u(t, x)) \left[ \frac{(\gamma^h - \gamma^l)}{(v^h - v^l)} (u(t, x) - v^h) + \gamma^h \right]. \end{aligned}$$

The terminal condition is  $u(T, x) = g(x)$ , where  $g(x) = \min\{x_1, \dots, x_d\}$ .

### 2.3. Hamilton-Jacobi-Bellman (HJB) equation

Another type of nonlinear parabolic PDE is the HJB equation with its variables defined on Eq. (1). In dynamic programming, particularly in game theory with multiple players, each player needs to solve the HJB equation to determine an optimal strategy. Consider the stochastic dynamical model

$$dX_t = 2\sqrt{\lambda}\mathcal{M}_t dt + \sqrt{2}dW_t, \quad (8)$$

where  $X_t$  is a state process,  $\{W_t\}$  is a Wiener process,  $\{\mathcal{M}_t\}$  is a control process, and  $\lambda$  is a strength of the control with  $t \in [0, T]$  and  $X_0 = x \in \mathbb{R}^d$ . The objective of a control problem in a classical linear-quadratic Gaussian (LQG) is to minimize a cost functional

$$J(\{\mathcal{M}_t\}_{0 \leq t \leq T}) = \mathbb{E} \left[ \int_0^T \|\mathcal{M}_t\|^2 dt + g(X_T) \right].$$

The aforementioned control problem can be written as an HJB equation for  $d$  dimension

$$\frac{\partial u}{\partial t}(t, x) + \Delta_x u(t, x) = \lambda \|(\nabla_x u)(t, x)\|^2. \quad (9)$$

Considering a terminal condition  $u(T, x) = g(x)$  for  $x \in \mathbb{R}^d$ , an explicit solution of Eq. (9) can be written as

$$u(t, x) = -\frac{1}{\lambda} \ln \left( \mathbb{E} \left[ \exp(-\lambda g(x + \sqrt{2}W_{T-t})) \right] \right) \quad (10)$$

with

$$g(x) = \ln \left( \frac{1 + \|x\|^2}{2} \right). \quad (11)$$

For the case studied in this paper, we use the same number of assets in [1] and extend it to a higher dimension.

### 2.4. The Deep-BSDE Method

This section provides a brief overview of the deep-BSDE method, as outlined in [1], to offer an insight about how the method works. To numerically solve the BSDE in Eq. (3), our primary objective is to determine  $u(0, X_0)$ , such that the value of  $u(t_N, X_{t_N})$  calculated using Eq. (5) closely approximates the terminal condition  $g(X_{t_N})$ . Additionally, calculation of the value of  $u(t_N, X_{t_N})$  depends on the unknown values of  $\nabla u(t_n, X_{t_n})$  for  $n = 0, \dots, N-1$ . To estimate the value of  $u(0, X_0)$ , we adopt the deep-BSDE approach in [1], which has been shown to solve BSDE better than other traditional numerical methods. In general, we will update weight parameters inside the deep neural networks as:

$$\boldsymbol{\theta} = \{\theta_{u_0}, \theta_{\nabla u_0}, \theta_1, \dots, \theta_{N-1}\},$$

where  $\theta_{u_0} \approx u(0, X_0)$ ,  $\theta_{\nabla u_0} \approx \nabla u(0, X_0)$ .

At the top level of deep neural network, the initial guess of  $\theta_{u_0}$  is selected randomly from a certain interval  $[a, b]$  which is set to be not far from the actual value  $u(0, X_0)$ .

Based on Eqs. (4)-(6), the deep neural network estimates  $u(t_N, X_{t_N})$  by optimizing the weight parameters  $\theta$  in terms of a loss function  $\ell$ . In that case, we minimize the loss function  $\ell$ , which is defined by

$$\ell(\theta, \{X_{t_n}\}, \{\Delta W_{t_n}\}) = \mathbb{E} (\|g(X_{t_N}) - u(t_N, X_{t_N})\|^2). \quad (12)$$

The above loss function represents the difference of  $u(t_N, X_{t_N})$  with the terminal condition  $g(X_{t_N})$  of the PDE. Then the deep-BSDE method optimizes all weights in the network using the stochastic gradient descent-type (SGD) algorithm simultaneously. Note that, the one we need the most is the solution of Eq. (1) or (3) which is represented by  $\theta_{u_0}$  as an approximation of  $u(0, X_0)$ .

### 3. Deep Genetic Algorithm (Deep-GA)

In this research, we propose to combine GA with deep learning techniques, resulting in a novel approach that we refer to as the deep genetic algorithm (deep-GA). We embed the GA as an optimization procedure into the well-cited deep-BSDE solver with the expectation of enhancing its efficiency. Unlike other methods, such as the shooting method [34], the GA is capable of handling the weights of deep-BSDE and the stochastic differential equations. The embedding accelerates the convergence for calculating  $u_0$  while simultaneously widening the interval for determining the initial guess  $u_0$ .

As mentioned earlier, the deep-BSDE method introduced in [1] requires an initial guess of  $\theta_{u_0}$  as the approximation of  $u_0$ , drawn from a certain interval  $[a, b]$ . This  $\theta_{u_0}$  represents the solution of the PDE, distinct from the general weights of neural networks  $\{\theta_{\nabla u_0}, \theta_1, \dots, \theta_{N-1}\}$ . Determining the appropriate value for the initial approximation,  $\theta_{u_0}$ , proves to be a challenging task without precise knowledge regarding the discussed problem's actual value. Our preliminary studies (in Section 4.1) found that the initial guess of  $\theta_{u_0}$  plays an important role in the solution process. When  $\theta_{u_0}$  is too far from the actual value, the method might need prolonged iterations to converge or, in some cases, fail to converge altogether. Consequently, finding a good initial guess is essential in the deep-BSDE method.

In our proposed method, we create a population of possible solutions to approximate  $u_0$  instead of using only one weight  $\theta_{u_0}$  in the original deep-BSDE method. The population is subsequently optimized using the GA, while the remaining weights are updated using the Adam optimizer akin to the process in the deep-BSDE method. A detailed illustration of the deep-GA scheme is provided in Fig. 1.

#### 3.1. Initialization and generating population

The deep-GA begins by determining several important parameters, including the number of chromosomes ( $m$ ), the number of generations ( $b$ ), the probability of crossover ( $p_c$ ), the probability of mutation ( $p_m$ ), the minimum value of  $u_0$  ( $\min(u_0)$ ), and the maximum value of  $u_0$  ( $\max(u_0)$ ). The parameters employed in this study are  $m = 10$ ,  $b = 10$ ,  $p_c = 0.8$ ,  $p_m = 0.4$ ,  $\min(u_0) = 0$ ,  $\max(u_0) = 100$  for the BS equation case, and  $\max(u_0) = 10$  for the HJB equation case. Notably, the interval  $[\min(u_0), \max(u_0)]$  used for obtaining the initial guess of  $u_0$  is broader than the one used in the deep-BSDE method.

Next, a population  $\{u_{0_1}, u_{0_2}, \dots, u_{0_m}\}$  consisting of  $m$  different possible solutions of  $u_0$  is generated. The solutions are selected from the interval  $[\min(u_0), \max(u_0)]$  using

$$u_{0_i} = \min(u_0) + \frac{i}{m}(\max(u_0) - \min(u_0)) \quad (13)$$

for  $i = 1, 2, \dots, m$ . Equation (13) will give us a population consisting of solutions which are evenly distributed over the interval. To ensure stability in our results, three separate populations are generated in the beginning of the deep-GA method. Genetic operators will evolve these populations without any interactions among them. The final value of  $u_0$  is taken to be the average of all chromosomes from the three populations.

### 3.2. Selection, crossover, and mutation operators

To produce new approximations for  $u_0$  from the population  $\{u_{0_1}, u_{0_2}, \dots, u_{0_m}\}$ , the GA uses selection, crossover, and mutation operators. Each operator has a different role in obtaining new approximations. In general, the selection is utilized to pair solutions that will be used as inputs in the subsequent steps. Crossover combines existing solutions to facilitate convergence within a region, while mutation is employed to escape local optima [35].

The deep-GA method uses a random selection by choosing a pair of solutions from the initial population. Let  $(v_1, v_2)$  represent the selected pair. With probability  $p_c$ , a new solution  $v$  will be produced by crossover which is calculated as

$$v = \frac{1}{2}(v_1 + v_2). \quad (14)$$

Next, the mutation is applied to each solution  $u_{0_i}$  in the initial population with probability  $p_m$  and a new solution  $w$  produced is calculated as

$$w = u_{0_i} + \varepsilon \left( \frac{\max(u_0) - \min(u_0)}{100} \right), \quad (15)$$

where  $\varepsilon$  is randomly selected from the interval  $[-1, 1]$ .

In addition to the aforementioned mutations, we also compute four new solutions namely

$$y_j = \bar{u}_0 + \alpha_j \left( \frac{\max(u_0) - \min(u_0)}{100} \right), \quad (16)$$

where  $j = 1, \dots, 4$ ,  $\alpha_1 = 1$ ,  $\alpha_2 = -1$ ,  $\alpha_3 = 2$ ,  $\alpha_4 = -2$ , and  $\bar{u}_0$  is the average of all solutions  $u_{0_i}$ ,  $i = 1, \dots, m$ , in the initial population.

Selection, crossover, and mutation processes are performed  $m$  times, corresponding to the number of solutions in the initial population. The crossover and mutation are controlled by two parameters  $p_c$  and  $p_m$  and the expected number of new solutions produced is  $[(p_c + p_m)m] + 4$ . Combining with the initial population, we would have about  $[(p_c + p_m + 1)m] + 4$  solutions in the current population.

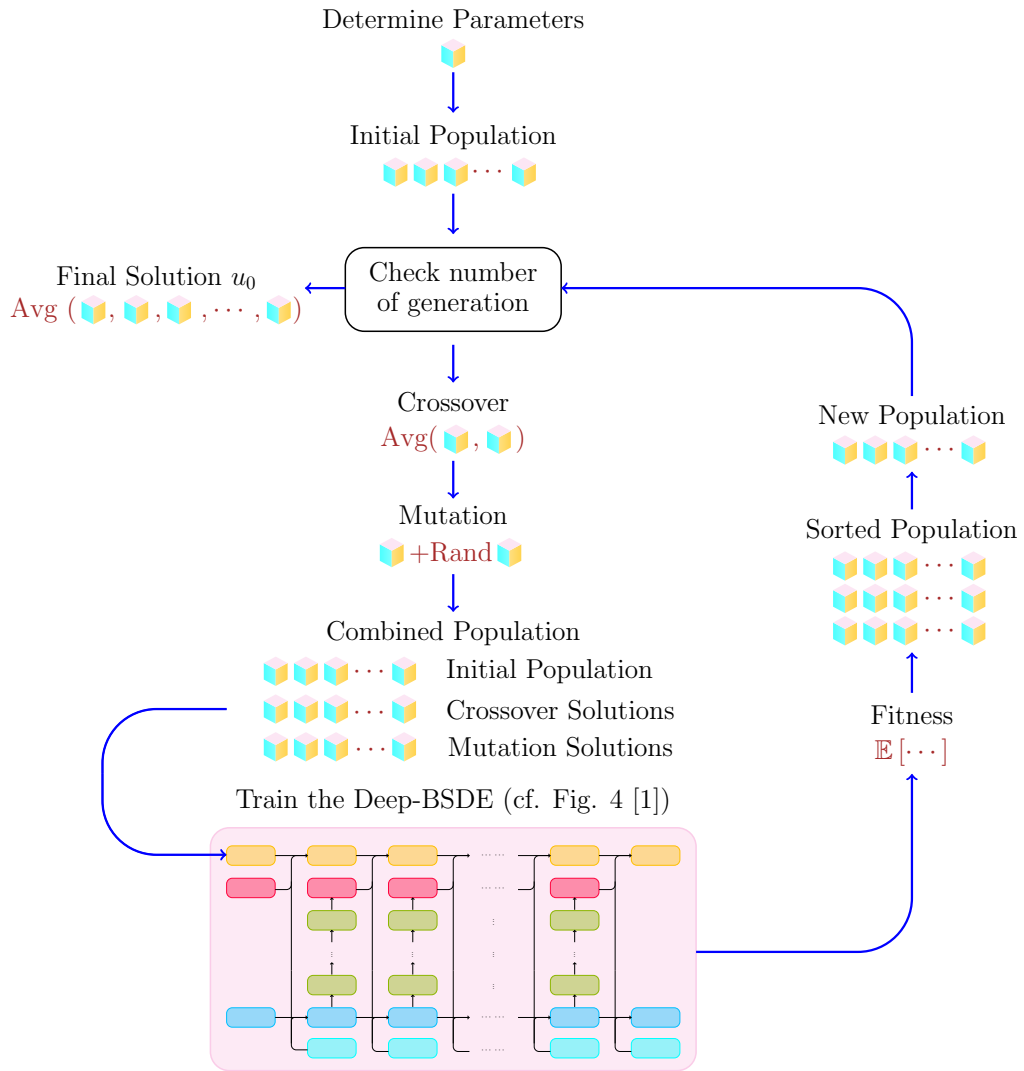


Figure 1: Scheme of the deep-GA method.



### 3.3. Deep neural network and fitness function

A fitness function is required to assess the fitness value of each solution  $u_{0_i}$ ,  $i = 1, \dots, m$ , to determine which solutions are superior to others. To define the fitness function, we use a similar deep neural network with the same weights  $\boldsymbol{\theta} = \{\theta_{u_0}, \theta_{\nabla u_0}, \theta_1, \dots, \theta_{N-1}\}$  as those utilized in the deep-BSDE method. In our proposed method, we optimize  $\theta_{u_0}$  using the GA and optimize  $\{\theta_{\nabla u_0}, \theta_1, \dots, \theta_{N-1}\}$  using an SGD-type algorithm. The optimization processes are carried out alternately.

First, we set the weight  $\theta_{u_0}$  with the average of all solutions from the current three populations. The network is then trained for  $p$  times (iterations) in each generation using the Adam optimizer. Even though at this step  $\theta_{u_0}$  is also updated, the value will be discarded and not used. In order to calculate the fitness value of  $u_{0_i}$ , we assign and replace the weight  $\theta_{u_0}$  in the network with  $u_{0_i}$ . Then the fitness function of the deep-GA is defined similarly to Eq. (12), but with a conditional weight as follows,

$$f(u_{0_i}, \boldsymbol{\theta}, \{X_{t_n}\}, \{\Delta W_{t_n}\}) = \mathbb{E}(\|g(X_{t_N}) - u(t_N, X_{t_N})\|^2 \mid \theta_{u_0} = u_{0_i}). \quad (17)$$

When calculating the fitness values of  $u_{0_i}$ , for  $i = 1, \dots, m$ , the other weights  $\{\theta_{\nabla u_0}, \theta_1, \dots, \theta_{N-1}\}$  remain unchanged. In this work, the fitness function is the same as that from Han et al. [1], i.e., Eq. (12). The conditional weights in the fitness function are selected to determine the value of  $\theta_{u_0}$  and obtain a precise fitness value for  $u_{0_i}$ .

The deep-GA method only uses a single deep neural network and shares its weights across all solutions  $u_{0_i}$  in the population. These processes are repeated in each generation. Since the deep-GA method consists of  $b$  generations, the network is trained for a total of  $pg$  iterations. The value of  $p$  can be chosen from [100, 1000].

### 3.4. New population and final solution

After completing all the aforementioned stages, it is necessary to sort the solutions in the population based on their fitness values from Eq. (17). The top  $m$  solutions will continue as the new population, while the remaining solutions are eliminated. All the processes in the deep-GA method are repeated for  $b$  generations. Finally, the solution  $u_0$  of the BSDEs, obtained by the deep-GA method, is the average of all solutions from the three populations.

Pseudo-code and scheme of the deep-GA method are illustrated in Fig. 1 and Algorithm 1. Note that for simplicity, the scheme in Fig. 1 is only using one population, instead of three. The code used for calculating the fitness function in the deep-GA is sourced from [1, 36]. Our code is based on the BSDE solver [1] and is available at [37]. We compiled the deep-BSDE and the deep-GA using Google Collaboratory.

## 4. Results and Discussions

### 4.1. Preliminary study

First, we demonstrate the search for solutions of the BS equation using the deep-BSDE method with various initial guesses of  $\theta_{u_0}$ . All settings used in the simulation follow [1] and the network is trained for 6000 iterations. Figure 2 shows that when the initial guess of  $\theta_{u_0}$  is significantly far from the actual value, the convergence of  $u_0$  is slow. In fact, convergence cannot be achieved within 6000 iterations for such initial guesses. Thus, the selection of the initial guess plays a crucial role in the solution process.

---

**Algorithm 1:** Pseudo-code of the deep-GA method.

---

**Input:**  $m, b, p_c, p_m, \min(u_0), \max(u_0), \alpha_1, \alpha_2, \alpha_3, \alpha_4$  ;  
**Output:**  $u_0$  ;  
 $P_1 \leftarrow \text{GeneratePopulation}(\max(u_0), \min(u_0), m)$  ;  
 $P_2 \leftarrow \text{GeneratePopulation}(\max(u_0), \min(u_0), m)$  ;  
 $P_3 \leftarrow \text{GeneratePopulation}(\max(u_0), \min(u_0), m)$  ;  
**for** generation = 1 :  $b$  **do**  
  **for**  $l = 1 : 3$  **do**  
     $\bar{u}_0 \leftarrow \text{Average}(P_l)$  ;  
    **for**  $i = 1 : m$  **do**  
      **if**  $\text{Random}([0, 1]) < p_c$  **then**  
         $v_1 \leftarrow \text{RandomSelection}(P_l)$  ;  
         $v_2 \leftarrow \text{RandomSelection}(P_l)$  ;  
         $v \leftarrow \frac{1}{2}(v_1 + v_2)$  ;  
         $P_l \leftarrow \text{Append}(P_l, v)$  ;  
      **end**  
      **if**  $\text{Random}([0, 1]) < p_m$  **then**  
         $\varepsilon \leftarrow \text{Random}([-1, 1])$  ;  
         $w \leftarrow u_{0_i} + \varepsilon \left( \frac{\max(u_0) - \min(u_0)}{100} \right)$  ;  
         $P_l \leftarrow \text{Append}(P_l, w)$  ;  
      **end**  
    **end**  
    **for**  $j = 1 : 4$  **do**  
       $y_j \leftarrow \bar{u}_0 + \alpha_j \left( \frac{\max(u_0) - \min(u_0)}{100} \right)$  ;  
       $P_l \leftarrow \text{Append}(P_l, y_j)$  ;  
    **end**  
  **end**  
   $\theta_{u_0} \leftarrow \text{Average}(P_1, P_2, P_3)$  ;  
  **for**  $i = 1 : p$  **do**  
     $\{X_{t_n}\}, \{\Delta W_{t_n}\} \leftarrow \text{GenerateSample}(\mu, \sigma, \Delta t)$  ;  
     $\theta \leftarrow \text{Train}(\theta, \{X_{t_n}\}, \{\Delta W_{t_n}\})$  ;  
  **end**  
   $\{X_{t_n}\}, \{\Delta W_{t_n}\} \leftarrow \text{GenerateSample}(\mu, \sigma, \Delta t)$  ;  
  **for**  $l = 1 : 3$  **do**  
    **for**  $i = 1 : \text{Size}(P_l)$  **do**  
       $\theta_{u_0} \leftarrow u_{0_i}$  ;  
      fitness  $\leftarrow f(u_{0_i}, \theta, \{X_{t_n}\}, \{\Delta W_{t_n}\})$  ;  
       $F_l \leftarrow \text{Append}(F_l, \text{fitness})$  ;  
    **end**  
  **end**  
   $P_l, F_l \leftarrow \text{Sort}(P_l, F_l)$  ;  
   $P_l \leftarrow \text{Eliminate}(P_l, m)$  ;  
**end**  
 $u_0 \leftarrow \frac{1}{3}(\text{Average}(P_1) + \text{Average}(P_2) + \text{Average}(P_3))$  ;

---

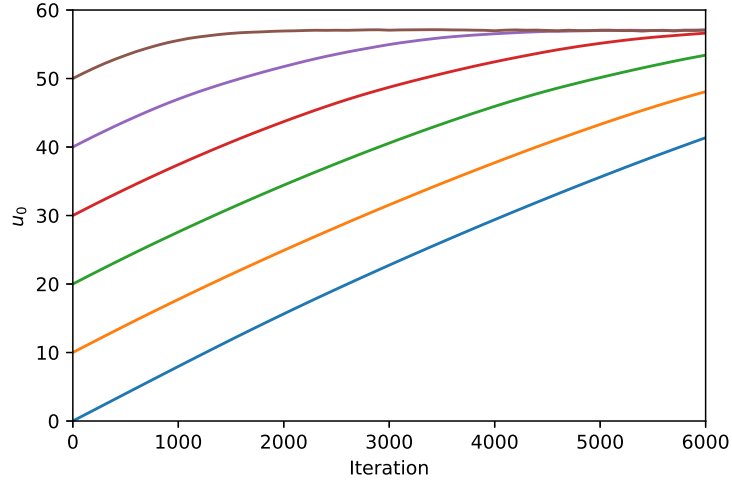


Figure 2: Plot of  $u_0$  obtained from the deep-BSDE method in 6000 iterations for six different initial guesses of  $u_0$ .

Table 1: Loss values of the deep-BSDE method for different initial guesses of  $\theta_{u_0}$  from five independent runs without any weight training - the nonlinear - BS equation with default risk.

$\theta_{u_0}$	Loss					Average	Std
	1	2	3	4	5		
0	3682.33	3581.65	3678.51	3677.77	3723.98	3668.85	52.43
10	2491.00	2488.57	2488.68	2466.36	2503.04	2487.53	13.26
20	1525.25	1564.84	1560.57	1558.50	1526.19	1547.07	19.63
30	786.31	796.03	787.36	815.15	815.17	800.00	14.34
40	312.10	330.30	324.18	307.54	323.30	319.48	9.36
50	72.55	67.43	72.57	67.86	64.30	68.94	3.58
60	34.30	40.71	27.08	32.05	28.79	32.59	5.34
70	146.43	147.19	155.63	148.78	173.33	154.27	11.25
80	473.34	484.84	513.87	487.00	511.87	494.18	17.84
90	1013.13	1012.78	1013.73	1079.93	1068.09	1037.53	33.56
100	1772.72	1812.55	1782.69	1824.90	1798.66	1798.31	21.26

Table 2: Loss values of the deep-BSDE method for different initial guesses of  $\theta_{u_0}$  from five independent runs without any weight training - the HJB equation.

$\theta_{u_0}$	Loss					Average	Std
	1	2	3	4	5		
0	19.821	19.512	19.565	19.485	19.992	19.675	0.198
1	11.725	11.821	11.941	11.536	11.732	11.751	0.133
2	5.801	6.149	5.965	6.037	6.021	5.995	0.114
3	2.086	2.034	2.096	2.168	2.087	2.094	0.043
4	0.232	0.208	0.225	0.231	0.262	0.232	0.017
5	0.414	0.360	0.349	0.420	0.348	0.378	0.032
6	2.492	2.511	2.483	2.535	2.564	2.517	0.030
7	6.575	6.526	6.588	6.721	6.674	6.617	0.071
8	12.746	13.037	12.840	12.500	12.770	12.779	0.173
9	20.578	21.118	20.889	20.684	21.128	20.879	0.223
10	31.104	30.949	31.036	31.141	31.015	31.049	0.068

Secondly, we illustrate the significance of selecting initial guesses for  $\theta_{u_0}$  during the first iteration of deep-BSDE. Each initial guess is compiled in five independent runs to demonstrate that the random weights of deep-BSDE in each run have minimal impact on the loss values, while the choice of  $\theta_{u_0}$  does. The results are presented in Table 1 and Table 2. The loss values of all independent runs have relatively small changes compared to the averages for each  $u_0$  value. As indicated by the standard deviations, when the initial guess  $\theta_{u_0}$  is closer to the actual values, the loss values are smaller. This indicates that to enhance efficiency, it is important to select  $\theta_{u_0}$  with greater accuracy.

#### 4.2. Non-linear Black-Scholes equation with default risk

The fair price of the European multi asset contingent claim, as governed by the nonlinear BS equation with default risk in Eq. (3), has been simulated using both our proposed deep-GA and the deep-BSDE methods. For the simulations, we use parameters in [1], i.e.,  $r = 0.02$ ,  $\delta = 2/3$ ,  $\gamma_h = 0.2$ ,  $\gamma_l = 0.02$ ,  $\hat{\mu} = 0.02$ ,  $v_h = 50$ , and  $v_l = 70$ . We assume that  $d = 100$  assets have uniform price  $x = \{100, 100, \dots, 100\}$  with uniform volatility values  $\hat{\sigma}$  for each asset. It is important to note that the volatility  $\sigma$  is a  $d \times d$  matrix for each value (see Eq. (1)) but here we use  $\hat{\sigma}$  for simulation based on Eq. (7). The connection between  $\sigma$  and  $\hat{\sigma}$  has been explained in Section 2.2. In addition, we range the values of volatility used in the simulation  $\hat{\sigma} \in \{0.1, 0.5\}$  to show the effect of volatility to the value of the European contingent claim. The parameters of GA are also determined following [1]: learning rate = 0.008, batch size = 64, and validation size = 256. For the deep-BSDE method, we choose a single value from an interval [40, 50] as the initial guess value of  $\theta_{u_0}$  and the model is trained for 10000 times. For the deep-GA method, we use  $g = 15$ ,  $p = 100$ , and hence the model is trained 1500 times in total.

We compare the results obtained by the deep-GA and the deep-BSDE methods for various values of  $\hat{\sigma}$  in Table 3. Following [16, 38], we will take the values of  $u_0$  obtained using Picard method as “the actual values”. The results from the deep-GA method exhibit strong agreement with the “actual values”, and the absolute percentage error is comparable to that of the deep-BSDE.

Various values of volatility  $\hat{\sigma}$  represent changes in assets’ rate of returns, leading to increased complexity in the pricing process. The price of contingent claim  $u(x, t)$  is de-

Table 3: Results obtained by the deep-BSDE and the deep-GA for different values of  $\hat{\sigma}$ .

$\hat{\sigma}$	$u_0$			Abs. Percentage Error		Time	
	Picard	Deep-BSDE	Deep-GA	Deep-BSDE	Deep-GA	Deep-BSDE	Deep-GA
0.1	77.00	76.88	76.95	0.156	0.065	1386	759
0.2	57.32	56.99	57.07	0.576	0.436	1351	736
0.3	42.50	42.24	42.05	0.612	1.059	1350	749
0.4	32.12	31.63	31.94	1.526	0.560	1348	775
0.5	24.09	23.50	23.38	2.449	2.947	1436	775

Table 4: Comparison of the deep-BSDE and the deep-GA for different numbers of dimension - the nonlinear BS equation with default risk.

$d$	$u_0$			Abs. Percentage Error		Time	
	Picard	Deep-BSDE	Deep-GA	Deep-BSDE	Deep-GA	Deep-BSDE	Deep-GA
100	77.00	76.88	76.95	0.156	0.065	1386	759
200	75.16	75.08	75.24	0.106	0.093	2315	1064
300	74.18	74.12	74.06	0.081	0.162	3340	1295
400	73.53	73.48	73.41	0.068	0.163	4438	1444
500	72.99	72.97	72.98	0.027	0.014	5571	1632

terminated by solving Eq. (3). As  $\hat{\sigma}$  increases, the task determining the initial guess of  $\theta_{u_0}$  becomes increasingly complicated, resulting in longer computational times. However, our deep-GA shows a higher efficiency than that of the deep-BSDE method as the volatility  $\hat{\sigma}$  increases.

To show the high-dimensional effect to the solution process of the BS equation, we present some numerical results in Table 4. As the dimension increases, the computational time for both methods increases. Nevertheless, the deep-GA has a half rate of computational time increment than that of the deep-BSDE in average. Therefore, the deep-GA is more efficient in solving the PDE than the deep-BSDE.

Furthermore, we present in Figs. 3 and 4 the convergence of the estimated solutions  $u_0$  and the losses for  $\hat{\sigma} = 0.1$  in the first 750 seconds of both methods, respectively. In the case of the deep-GA method, the solutions  $u_0$  and the loss values plotted in the figures represent the average of all solutions and the averages of all fitness values across the three populations. One can observe the fast convergent of the solution computed using our proposed method. Although losses from both methods started with nearly identical initial values, the loss of the deep-GA method decreases rapidly in the first 200 seconds.

#### 4.3. Hamilton-Jacobi-Bellman (HJB) equation

In this subsection, we simulate an HJB equation for the minimum cost of an optimal strategy in investments. For simulations, we use  $\lambda \in \{1, 10, 20, 30, 40, 50\}$ , learning rate = 0.01, batch size = 64, and validation size = 256. For the deep-BSDE method, we choose a random value from the interval  $[7, 8]$  as an initial guess of  $\theta_{u_0}$  and then the model is trained for 40000 times, while for the deep-GA method, we use  $b = 20$ ,  $p = 1000$ , resulting in a total of 20,000 training iterations.

The results obtained from both the deep-BSDE and deep-GA methods for various values of the control strength  $\lambda$  are presented in Table 5. We compare these results with those obtained using the Monte Carlo method, as reported in [1]. Assuming Monte

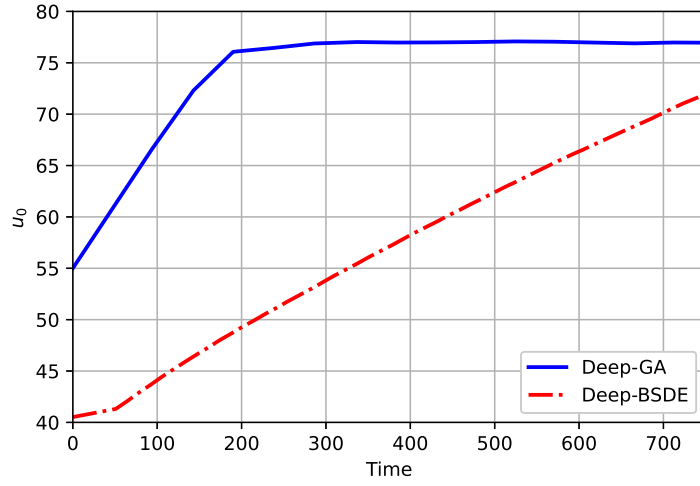


Figure 3:  $u_0$  of the BS equation against time for  $\hat{\sigma} = 0.1$  in the first 750 seconds.

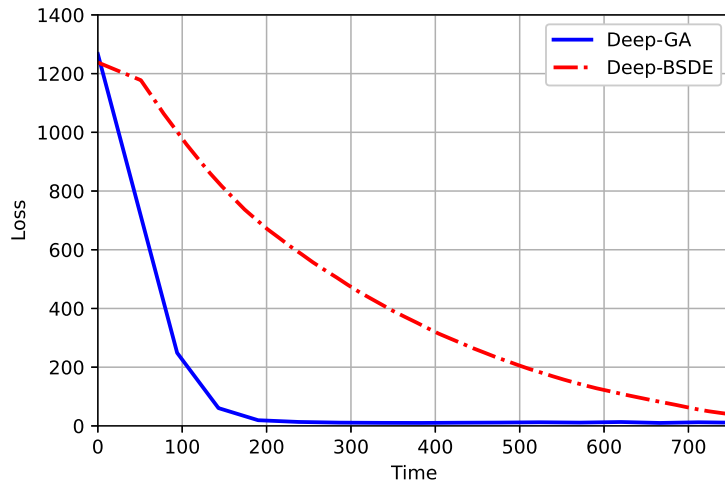


Figure 4: Loss in the BS equation against time for  $\hat{\sigma} = 0.1$  in the first 750 seconds.

Table 5: Results obtained by the deep-BSDE and the deep-GA for different values of  $\lambda$ .

$\lambda$	$u_0$			Abs. Percentage Error		Time	
	Monte Carlo	Deep-BSDE	Deep-GA	Deep-BSDE	Deep-GA	Deep-BSDE	Deep-GA
1	4.590	4.606	4.596	0.349	0.131	2531	1530
10	4.493	4.503	4.508	0.223	0.334	2680	1512
20	4.369	4.415	4.416	1.053	1.076	2658	1495
30	4.247	4.370	4.350	2.896	2.425	2691	1483
40	4.158	4.295	4.281	3.295	2.958	2645	1506
50	4.096	4.241	4.212	3.540	2.832	2706	1504

Table 6: Comparison of the deep-BSDE and the deep-GA for different numbers of dimension - the HJB equation.

$d$	$u_0$			Abs. Percentage Error		Time	
	Monte Carlo	Deep-BSDE	Deep-GA	Deep-BSDE	Deep-GA	Deep-BSDE	Deep-GA
100	4.590	4.606	4.596	0.349	0.131	2531	1530
200	5.291	5.296	5.296	0.095	0.095	4225	1740
300	5.699	5.706	5.697	0.123	0.035	5776	2406
400	5.988	5.983	5.985	0.084	0.050	7695	2523
500	6.212	6.220	6.211	0.129	0.016	9859	2943

Carlo method provides “actual results”, the solution obtained by the deep-GA is fairly comparable to that obtained by the deep-BSDE method but with significantly less computational time. The use of the GA in the deep-GA method for optimizing the search of the initial guess value noticeably enhances the efficiency compared to the former method described in [1].

For various numbers of dimension  $d$ , the computational times of both deep-GA and deep-BSDE to solve the HJB equation increase as the dimension is higher. The rate of computational time increase of the deep-GA is also approximately half of the deep-BSDE in average. The results for the HJB equation are consistent with those for the BS equation (see Eqs.(7) and (9)). Moreover, the percentage error of the deep-GA also follows the same trend on average with that of the deep-BSDE (see Table 6) .

In Figs. 5 and 6, we show the trajectories of the estimated solutions  $u_0$  and the associated losses for  $\lambda = 50$  in the first 1500 seconds from both methods. Notably, the solutions of the deep-BSDE method decrease faster only in the first 150 seconds. Beyond that, the deep-GA method demonstrates superiority and rapid convergence. This pattern is also reflected in the movement of losses for both methods. Despite using the same learning rate, the loss of the deep-BSDE method displays noticeable fluctuations while the one of the deep-GA methods remains stable. Full detailed results of different parameters from both methods for the BS and HJB cases are provided at [37].

## 5. Conclusion

In this research, we introduced a novel method for solving high-dimensional and nonlinear PDEs, namely the deep-GA method. We applied this method to estimate the solution  $u_0$  of BSDEs associated with two nonlinear PDEs: the BS equation with default risk and the HJB equation, considering various parameters. The results obtained using

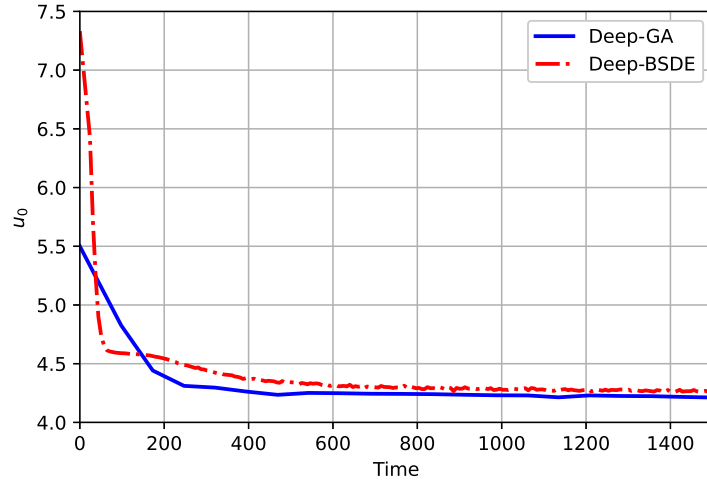


Figure 5:  $u_0$  of the HJB equation against time for  $\lambda = 50$  in the first 1500 seconds.

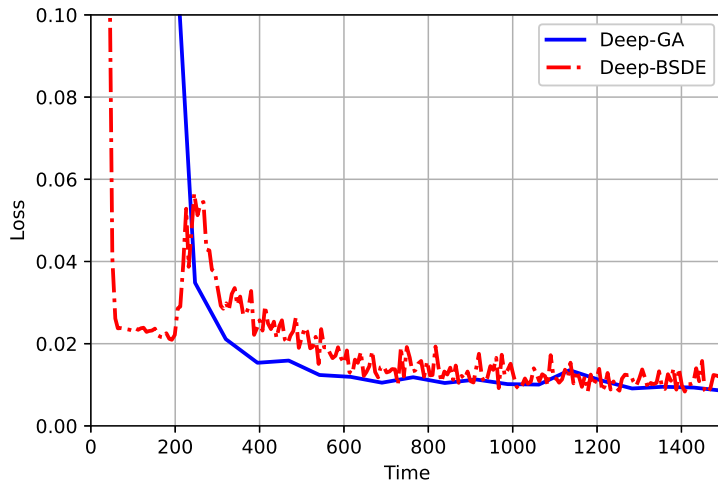


Figure 6: Loss of the HJB equation against time for  $\lambda = 50$  in the first 1500 seconds.



this method for both equations demonstrate good agreement with the actual values obtained from Picard and Monte Carlo methods. Furthermore, the deep-GA method exhibits significantly efficient computational times compared to the deep-BSDE method.

We have demonstrated that giving careful consideration to the choice of the initial guess for  $\theta_{u_0}$  rather than solely focusing on updating weights of the hidden layers is critical. This approach provides a broad and flexible way to determine the initial guess interval, resulting in a fast convergence rate compared to the deep-BSDE method. Furthermore, our proposed method can offer effective suggestions even when the ideal interval for the initial guess of  $\theta_{u_0}$  is unknown. We believe that this method can be applied to solve other problems where one or more weights play a more significant role than others. For future work, a jump-diffusion case might be considered to represent the existence of small and continuous price changes and large and infrequent ones represented by Poisson process, simultaneously.

## 6. Acknowledgement

This work was funded by the Ministry of Education, Culture, Research, and Technology of the Republic Indonesia through the World Class Professor Program year 2021. H.S. also acknowledges support from Khalifa University through a Faculty Start-Up Grant (No. 8474000351/FSU-2021-011) and a Competitive Internal Research Awards Grant (No. 8474000413/CIRA-2021-065).

## References

- [1] J. Han, A. Jentzen, E. Weinan, Solving high-dimensional partial differential equations using deep learning, *Proceedings of the National Academy of Sciences* 115 (34) (2018) 8505–8510.
- [2] M. Bernhart, H. Pham, P. Tankov, X. Warin, Swing options valuation: A BSDE with constrained jumps approach, in: *Numerical methods in finance*, Springer, 2012, pp. 379–400.
- [3] N. Esmaceli, P. Imkeller, et al., American options with asymmetric information and reflected BSDE, *Bernoulli* 24 (2) (2018) 1394–1426.
- [4] Z. Sun, X. Zhang, Y.-N. Li, A BSDE approach for bond pricing under interest rate models with self-exciting jumps, *Communications in Statistics-Theory and Methods* 50 (14) (2021) 3249–3261.
- [5] F. Cordonì, L. Di Persio, Backward stochastic differential equations approach to hedging, option pricing, and insurance problems., *International Journal of Stochastic Analysis* (2014).
- [6] W. Liao, A. Q. Khaliq, High-order compact scheme for solving nonlinear Black-Scholes equation with transaction cost, *International Journal of Computer Mathematics* 86 (6) (2009) 1009–1023.
- [7] M. Kohler, A. Krzyżak, N. Todorovic, Pricing of high-dimensional American options by neural networks, *Mathematical Finance: An International Journal of Mathematics, Statistics and Financial Economics* 20 (3) (2010) 383–410.
- [8] L. Goudenège, A. Molent, A. Zanette, Machine learning for pricing American options in high-dimensional Markovian and non-Markovian models, *Quantitative Finance* 20 (4) (2020) 573–591.
- [9] E. Weinan, J. Han, A. Jentzen, Algorithms for solving high dimensional PDEs: from nonlinear Monte Carlo to machine learning, *Nonlinearity* 35 (1) (2021) 278.
- [10] S. Kim, D. Jeong, C. Lee, J. Kim, Finite difference method for the multi-asset Black-Scholes equations, *Mathematics* 8 (3) (2020) 391.
- [11] K. Miyamoto, K. Kubo, Pricing multi-asset derivatives by finite-difference method on a quantum computer, *IEEE Transactions on Quantum Engineering* 3 (2021) 1–25.
- [12] R. Zhang, Q. Zhang, H. Song, An efficient finite element method for pricing American multi-asset put options, *Communications in Nonlinear Science and Numerical Simulation* 29 (1-3) (2015) 25–36.
- [13] T. J. Moroney, I. W. Turner, A finite volume method based on radial basis functions for two-dimensional nonlinear diffusion equations, *Applied mathematical modelling* 30 (10) (2006) 1118–1133.

- [14] M. Hutzenthaler, A. Jentzen, T. Kruse, et al., On multilevel Picard numerical approximations for high-dimensional nonlinear parabolic partial differential equations and high-dimensional nonlinear backward stochastic differential equations, *Journal of Scientific Computing* 79 (3) (2019) 1534–1571.
- [15] J. Han, A. Jentzen, et al., Deep learning-based numerical methods for high-dimensional parabolic partial differential equations and backward stochastic differential equations, *Communications in mathematics and statistics* 5 (4) (2017) 349–380.
- [16] E. Weinan, J. Han, A. Jentzen, Deep learning-based numerical methods for high-dimensional parabolic partial differential equations and backward stochastic differential equations, *Communications in Mathematics and Statistics* 5 (4) (2017) 349–380.
- [17] S. Becker, P. Cheridito, A. Jentzen, Deep optimal stopping, *The Journal of Machine Learning Research* 20 (1) (2019) 2712–2736.
- [18] S. Becker, P. Cheridito, A. Jentzen, T. Welti, Solving high-dimensional optimal stopping problems using deep learning, *European Journal of Applied Mathematics* 32 (3) (2021) 470–514.
- [19] Q. Chan-Wai-Nam, J. Mikael, X. Warin, Machine learning for semi-linear PDEs, *Journal of scientific computing* 79 (3) (2019) 1667–1712.
- [20] J. Han, J. Lu, M. Zhou, Solving high-dimensional eigenvalue problems using deep neural networks: A diffusion Monte Carlo like approach, *Journal of Computational Physics* 423 (2020) 109792.
- [21] DGM: A deep learning algorithm for solving partial differential equations, *Journal of Computational Physics* 375 (2018) 1339–1364.
- [22] C. Beck, E. Weinan, A. Jentzen, Machine learning approximation algorithms for high-dimensional fully nonlinear partial differential equations and second-order backward stochastic differential equations, *Journal of Nonlinear Science* 29 (4) (2019) 1563–1619.
- [23] C. Beck, S. Becker, P. Cheridito, A. Jentzen, A. Neufeld, Deep splitting method for parabolic PDEs, *SIAM Journal on Scientific Computing* 43 (5) (2021) A3135–A3154.
- [24] S.-T. Pan, M.-L. Lan, An efficient hybrid learning algorithm for neural network-based speech recognition systems on FPGA chip, *Neural Computing and Applications* 24 (2014) 1879–1885.
- [25] S. Ding, C. Su, J. Yu, An optimizing BP neural network algorithm based on genetic algorithm, *Artificial intelligence review* 36 (2011) 153–162.
- [26] H. Xu, H. Chang, D. Zhang, DLGA-PDE: Discovery of PDEs with incomplete candidate library via combination of deep learning and genetic algorithm, *Journal of Computational Physics* 418 (2020) 109584.
- [27] S. Bouktif, A. Fiaz, A. Ouni, M. A. Serhani, Optimal deep learning LSTM model for electric load forecasting using feature selection and genetic algorithm: Comparison with machine learning approaches, *Energies* 11 (7) (2018) 1636.
- [28] S. Kilicarslan, M. Celik, S. Sahin, Hybrid models based on genetic algorithm and deep learning algorithms for nutritional Anemia disease classification, *Biomedical Signal Processing and Control* 63 (2021) 102231.
- [29] Y. Kwon, S. Kang, Y.-S. Choi, I. Kim, Evolutionary design of molecules based on deep learning and a genetic algorithm, *Scientific reports* 11 (1) (2021) 17304.
- [30] S. Kalsi, H. Kaur, V. Chang, DNA cryptography and deep learning using genetic algorithm with NW algorithm for key generation, *Journal of medical systems* 42 (2018) 1–12.
- [31] H. M. Balaha, M. Saif, A. Tamer, E. H. Abdelhay, Hybrid deep learning and genetic algorithms approach (HMB-DLGAHA) for the early ultrasound diagnoses of breast cancer, *Neural Computing and Applications* 34 (11) (2022) 8671–8695.
- [32] S. S. Skandha, M. Agarwal, K. Utkarsh, S. K. Gupta, V. K. Koppula, J. S. Suri, A novel genetic algorithm-based approach for compression and acceleration of deep learning convolution neural network: an application in computer tomography lung cancer data, *Neural Computing and Applications* 34 (23) (2022) 20915–20937.
- [33] E. Pardoux, S. Peng, Backward stochastic differential equations and quasilinear parabolic partial differential equations, in: *Stochastic partial differential equations and their applications*, Springer, 1992, pp. 200–217.
- [34] R. L. Burden, J. D. Faires, A. M. Burden, *Numerical analysis*, Cengage learning, 2015.
- [35] X.-S. Yang, *Nature-inspired optimization algorithms*, Academic Press, 2020.
- [36] Deep BSDE solver in TensorFlow, <https://github.com/frankhan91/DeepBSDE>, accessed: 2021-11-16.
- [37] Deep-genetic algorithm (deep-ga), <https://github.com/luthfishahab/deepga>, accessed: 2021-11-16.
- [38] E. Weinan, M. Hutzenthaler, A. Jentzen, T. Kruse, On multilevel Picard numerical approximations for high-dimensional nonlinear parabolic partial differential equations and high-dimensional

nonlinear backward stochastic differential equations, *Journal of Scientific Computing* 79 (3) (2019) 1534–1571.